Chemical Physics Letters 577 (2013) 38–41

Contents lists available at SciVerse ScienceDirect

Chemical Physics Letters

journal homepage: www.elsevier.com/locate/cplett

# Matalon–Packter law for stretched helicoids formed in precipitation processes

Shibi Thomas [a], Ferenc Molnár [b], Zoltán Rácz [c], István Lagzi [d,*]

[a] Department of Physics, University of Calicut, Kerala, India
[b] Department of Physics, Applied Physics, and Astronomy, Rensselaer Polytechnic Institute, Troy, NY, USA
[c] Institute for Theoretical Physics, Eötvös University – HAS, Budapest, Hungary
[d] Department of Physics, Budapest University of Technology and Economics, Budapest, Hungary

ARTICLE INFO

*Article history:*
Received 29 March 2013
In final form 17 May 2013
Available online 25 May 2013

ABSTRACT

Helicoid-like precipitation structures emerging in the wake of reaction–diffusion fronts are studied experimentally as well as theoretically. We find that the helicoids are stretched, their local pitch behind the advancing front increases exponentially. We compare this result to the exponential increase of the band spacing in Liesegang phenomena. The spacing coefficient ($p$) characterizing the exponential increase satisfies the same Matalon–Packter law in both cases, i.e. $p \sim 1/a_0$ where $a_0$ is the initial concentration of the outer electrolyte in the experimental setup. Our experiments also reveal that, at the microstructure level, the helicoids are assembled from building blocks of micron-size achiral spherulites.



## 1. Introduction

Helical and helicoidal structures are common architectures in nature and in man-made systems such as inorganic crystals or nanohelices [1–5]. The formation of these inherently chiral patterns is an interesting and rather complex problem due to the symmetry breaking which takes place at some stage of their evolution. In our recent work [6] we showed that emergence of helicoids and helices in precipitation processes in the wake of a planar reaction–diffusion front is an intrinsic property of the system and (in contrast to coming from initial and boundary condition effects) it can be attributed to a sophisticated interplay among the noise, the moving front, and the unstable modes of the precipitation dynamics. Our findings reveal that the emergence of helicoidal and helical patterns is reproducible with a finite, well-defined probability depending on the parameters of the system such as the initial concentration of the outer and inner electrolytes, the temperature and the width of the system (see Figures 1 and 2 for the experimental setup). Remarkably, the trends in the observed probabilities could be reproduced by generalizing a model used earlier for explaining Liesegang phenomena [6].

The helicoids and helices are actually closely related to Liesegang patterns which are precipitation patterns emerging in the wake of reaction–diffusion fronts, but the precipitation zones are parallel to each other. The position of the bands, their width, and their time of appearance are well characterized for Liesegang patterns [7–9]. In particular, the distance between consecutive bands in regular Liesegang phenomenon increases as a geometrical series and it can be characterized by the so-called spacing coefficient, $p$, such that $x_{n+1} - x_n = px_n$, where $x_{n+1}$ and $x_n$ are the positions of two consecutive bands measured from the initial junction point of the electrolytes. This is the well-know spacing law which has been the focus of a large number of studies [8–10]. It has been shown experimentally that the spacing coefficient depends on the initial concentrations $a_0$ and $b_0$ of the outer and inner electrolytes, as described by the following relation (Matalon–Packter law) [11,12]:

$$p = f(b_0) + \frac{g(b_0)}{a_0}, \tag{1}$$

where $f$ and $g$ are weakly dependent (decreasing functions) of their arguments.

It is a natural question whether the method of characterization of bands can be extended to helices as well, where the distance between the bands is equivalent to the local pitch of the helices. Our aim with this letter is to suggest that the spacing law and the related Matalon–Packter law are valid for helices. This suggestion is supported by the accord between our numerical simulations and the experimental findings. We also examine the microstructure of precipitation helicoids in order to ascertain that the origin of macroscopic helices is in symmetry breaking and not the chirality of the microscopic building blocks.

## 2. Experimental

Our experiments concerned the $CuCl_2$ and $K_2CrO_4$ precipitation reaction in a 1% agarose gel according to the chemical reaction

* Corresponding author. Fax: +36 1 463 1896.
*E-mail address:* lagzi@vuk.chem.elte.hu (I. Lagzi).

0009-2614/$ - see front matter © 2013 Elsevier B.V. All rights reserved.
http://dx.doi.org/10.1016/j.cplett.2013.05.031

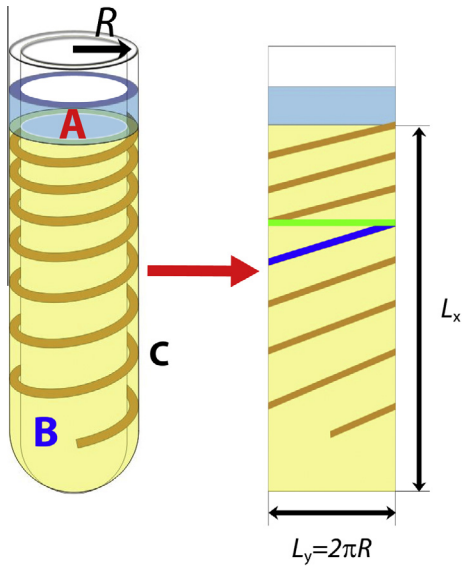


**Figure 1.** Transformation of the 3D experimental setup into a 2D domain used in numerical simulations. The unfolding of the cylinder onto the 2D domain ($L_x \times L_y$) requires that the boundary conditions are periodic in the horizontal direction, and the width of the domain $L_y$ is defined by the radius $R$ of the cylinder: $L_y = 2\pi R$. The single brown line (C) of helix in 3D corresponds to a set of tilted precipitation zones (lines) joined by the periodic boundary condition. Blue and yellow colors mark the regions where the reagents (A – outer electrolyte, B – inner electrolyte) are placed initially. (For interpretation of the references to colour in this figure legend, the reader is referred to the web version of this article.)

$Cu^{2+}(aq) + CrO_4^{2-}(aq) \rightarrow CuCrO_4(s)$ [13]. Agarose gel in a test tube contained potassium chromate as inner electrolyte was prepared by dissolving potassium chromate ($K_2CrO_4$, Sigma–Aldrich – the inner electrolyte) in double distilled water with the given amount of agarose powder (Type I, Sigma–Aldrich). The mixture was heated to 90 °C under constant stirring until a homogeneous solution was obtained. The resulting solution was then poured into test tubes of 16 mm diameters. After polymerization (2 h) a solution of copper chloride ($CuCl_2$, Sigma–Aldrich – the outer electrolyte) was gently poured on top of the potassium chromate-doped gel (see Figure 1 for the experimental setup). The pattern formation was monitored at room temperature (22.0 ± 0.3 °C) by a digital camera for 7 days. All experiments were carried out with much higher concentrations of the outer electrolyte ($CuCl_2$). Details of the experimental parameters used are described in Ref. [13]. Experimental results indicate that both the Liesegang bands and the helicoids/helices emerge in a wide range of the parameters. In general, we found that precipitation helicoids formed with higher probability when the concentration of the outer electrolyte was higher, thus ensuring fast motion of the front [6]. Noise (e.g., thermal) also plays a crucial role in helicoid formation, probability of the emergence of helicoids increases with the amplitude of the noise. Finally, the radius of the test tube also has the influential effect. The probability of helicoidal pattern formation increases with the radius of the test tube. Moreover, there is a critical radius, below which only Liesegang bands are formed regardless of the other parameters.

## 3. Numerical

Models of Liesegang phenomena use various aspects of pre- and post-nucleation dynamics. A theory that incorporates both dynamics through a phase separation scenario is based on the Cahn–Hilliard equation [14]. This description features fast, spinodal-decomposition type precipitation dynamics, as well as slower, nucleation-and-growth processes [15] and it can reproduce all the well-established laws related to Liesegang patterns (time-, spacing-, width-, and Matalon–Packter laws) [8–12].

We use the Cahn–Hilliard dynamics combined with reaction–diffusion equations which produce the reaction front where the particles for the precipitation are produced. Assuming an irreversible reaction A + B → C between the outer (A) and inner (B) electrolytes, the pattern formation phenomena in the gel is described by the following reaction–diffusion equations

$$\partial_t a = D\Delta a - kab \tag{2}$$

$$\partial_t b = D\Delta b - kab \tag{3}$$

$$\partial_t m = -\lambda\Delta\left(m - m^3 + \sigma\Delta m\right) + kab + \eta_c, \tag{4}$$

where $k$ is the reaction rate and, for simplicity, the diffusion coefficients ($D$) of the reagents are taken to be equal. $m$ is the shifted and appropriately scaled concentration of the precipitating particles (C). The front is described in terms of the spatio-temporal properties of $kab$ (rate of production of C's), and $\lambda$, $\sigma$, $\eta_c$ are the rescaled kinetic coefficient, surface tension, and conserved noise, respectively [6,16]. During the precipitation process the C particles segregate into low ($c_l$: m = −1) and high ($c_h$: m = 1) concentration states described by Eq. (4) (for the detailed model description see Refs. [6,16]). Eqs. (2)–(4) were solved by applying a 'method of lines' using spatial discretization on a rectangular grid followed by integration of the resulting ordinary differential equations by the forward Euler method. The conserved noise $\eta_c$ was realized by moving Cs to neighboring sites at a rate $\eta_c = r\sqrt{\bar{c}}$, where $r$ is a random number uniformly distributed in an interval $[-\eta, \eta]$ with $\eta$ characterizing the strength of the noise. The grid spacing and the time step were 1.0 and 0.02, respectively. We used periodic boundary conditions in the $y$ direction (see Figure 1 for the reason of periodicity) and no-flux boundary conditions at the lower edge of the gel ($x = L_x, y$). The boundary condition at the upper edge ($x = 0, y$) for $A$ is a Dirichlet boundary, according to the assumption that the concentration of the outer electrolyte is kept at a constant value $a(x = 0, y, t) = a_0/\bar{c}$, while Neumann (no-flux) boundaries are used for B and C. The outer electrolyte concentration ($a_0$) was scaled by $\bar{c} = (c_h + c_l)/2$ in both experiments and numerical simulations. As can be inferred from Figure 1, parallel zones and tilted lines in simulations correspond to regular Liesegang and helical patterns, respectively. Solving the above numerical model with various initial and external parameters allowed us to characterize the spacing coefficient of helices and to compare these data with the experimental findings.

## 4. Results and discussion

In our experiments, helicoidal patterns emerged in columns of gel placed in test tubes. In this setup a planar diffusion front of the outer electrolyte moves into the gel and, in general, produces a series of distinct precipitation disks which is called the regular Liesegang pattern (see Figure 2). However, using the same experimental conditions, helicoidal pattern can also evolve (with well-defined probability) showing the stochastic nature of this phenomenon. In order to compare the properties of regular and helicoidal patterns, we carried out at least 10 independent experiments at the same fixed parameters and conditions.

To investigate the Matalon–Packer law for the helicoids we need to generalize the concept of spacing coefficients for helices. This can be done by defining $x_n$ through the position of the $n$th crossing of the helix at a given $y$ (Figure 2), and then $x_{n+1}/x_n - 1 = p_n$ should converge to the spacing coefficient $p$ for large $n$ (plotting $x_{n+1}$ versus $x_n$ and determining the slope of fitted linear curve). Note, that helices are often characterized by their pitch. It